ISSN: 0067-2904

Powell-Eyring Fluid Peristaltic Transfer in an Asymmetric Channel and A Porous Medium under the Influence of A Rotation and an Inclined Magnetic Field

Rana Ghazi Ibraheem*, Liqaa Zeki Hummady
. Department of Mathematic, College of Science, University of Baghdad, Baghdad, Iraq,

Received: 16/10/2022 Accepted: 25/1/2023 Published: 30/12/2023

Abstract

In this article, we investigate the peristaltic flow of a Powell-Eyring fluid flowing in an asymmetrical channel with an inclining magnetic field through a porous medium, and we focus on the impact that varying rotation has on this flow. Long wavelength and low Reynolds number are assumed, where the perturbation approach is used to solve the nonlinear governing equations in the Cartesian coordinate system to produce series solutions. Distributions of velocity and pressure gradients are expressed mathematically. The effect of these parameters is discussed and illustrated graphically through the set of figures. To get these numerical results, we used the math program MATHEMATICA.

Keywords : Peristaltic flow, Powell- Eyring fluid, inclined magnetic felid, porous medium, and rotation.

نقل سائل باول أرينغ التمعجي في قناة غير متماثلة ووسط مسامي تحت تأثير الدوران والمجال المغناطيسي المائل.

رنا غازي ابراهيم* , لقاء زكي حمادي
قسم الرياضيات, كلية العلوم, جامعة بغداد, بغداد, العراق

الخلاصه :

في هذه المقالة ، نبحث في التدفق التمعجي لسائل باول آرينغ الذي يتدفق في قناة غير متناظرة مع مجال مغناطيسي مائل عبر وسط مسامي ، ونركز على تأثير الدوران المتغير على هذا التدفق. يُفترض الطول الموجي الطويل وعدد رينولدز المنخفض ، حيث يتم استخدام نهج الاضطراب لحل المعادلات الحاكمة غير الخطية في نظام الإحداثيات الديكارتية لإنتاج حلول متسلسلة. يتم التعبير عن توزيعات تدرجات السرعة والضغط رياضيًا. تمت مناقشة تأثير هذه المعلمات وتوضيحها بيانياً من خلال مجموعة الأرقام. للحصول على هذه النتائج العددية ، استخدمنا برنامج الرياضيات MATHEMATICA.

1. Introduction

Peristaltic pumping is a specific sort of pumping when a wide range of intricate rheological fluids can be readily moved from between two locations. This pumping principle is referred to as peristaltic. The ducts through which the fluid passes undergo intermittent involuntary constriction and then expand. As a result, the pressure gradient rises, causing the fluid to move

*Email: rana.ghazi1103a@sc.uobaghdad.edu.iq

forward. After Latham's groundbreaking work [1] and because of its use in physiological, engineering, and biological systems academics have become increasingly interested in the different applications of peristalsis. Because of its use in physiological, engineering, and biological systems, peristaltic transport has received significant attention in recent years. Generally, the peristaltic wave's circular contractions and the successive longitudinal contractions that occur during peristalsis are generated by the sinuses which propagate along the fluid-containing duct. This technique is the basis for several muscular tubes, including the gastrointestinal tract, fallopian tubes, bile ducts, ureters, esophageal tubes, and others. Moreover, non-Newtonian fluids are better than numerous industrial and physiological processes that use Newtonian fluids. Among the models of non-Newtonian fluids (which can exhibit various rheological effects), that can be accessed is Powell-Earing fluid. Although this model is more difficult mathematically than models of non-Newtonian fluids, it deserves more attention because of its distinct benefits. Numerous researchers have been interested in the Powell-Eyring fluid's peristaltic flow mechanism since it was studied by Hina and Mustafa and Hayat and Alsaedi [2], Hayat and Naseema and Rafiq and Fuad [3], Hayat and Ahmed [4], Hussain and Alvi and Latif and Asghar [5], and Ali and Liqaa [6]. The static magnetohydrodynamic flow and heat transfer of an Eyring-Powell fluid on an expansion plate with viscous dissipation were studied and numerically explained [7]. The exchange of thermal energy between different system components is referred to as heat transfer. However, the medium's physical characteristics and the separate compartments' temperatures affect the speed. In recent years, the authors in [8], [9] have been conducted about studying the effect of heat transport on non-Newtonian fluids. The problem of peristaltic transport of an incompressible non-Newtonian fluid in a tapered asymmetric channel is discussed in [10]. The engineering of peristaltic pumps, roller pumps, hose pumps, tube pumps, finger pumps, heart-lung machines, blood pump machines, and dialysis machines is based on peristalsis. These applications include the transportation of aggressive chemicals, high solid slurries, toxic (nuclear industries), and other materials. With regard to well-established problems of the stir of semi-conductive physiological fluids, such as blood and blood pump machines, magnetic drug forcing, and pertinent methods of human digestion, the advantage of applied magnetic field (MHD) on peristaltic efficacy is crucial. It is also helpful in treating gastroparesis, chronic constipation, and morbid obesity as well as magnetic resonance imaging (MRI), which is used to identify brain, vascular diseases, and tumors. A substance that has several tiny holes scattered throughout it is referred to as a porous medium. In riverbeds, fluid infiltration and seepage are sustained by flows over porous media. Important examples of flows through a porous material are those through the ground, water, and oil. Oil is trapped in rock formations like limestone and sandstone, which make up the majority of an oil reservoir [11]. Natural porous media can be found in many different forms, such as sand, rye bread, wood, filters, bread loaves, human lungs, and the gallbladder. Food processing, oxygenation, hemodialysis, tissue condition, heat convection for blood flow from tissues' pores, and radiation between the environment and its surface all depend on the action of heat transfer in the peristaltic repositioning of fluid [12]–[15]. The aforementioned processes all benefit from mass transfer; in particular, the mass transfer that occurs as nutrients diffuse from the blood into nearby tissues cannot be understated. Greater mass transfer participation is typical in the distillation, diffusion of chemical contaminants, membrane separation, and combustion processes. It should be observed that when heat and mass transfer occur simultaneously, a relationship between fluxes and driving potentials exists. However, the temperature gradient is what causes the gradients in mass flux and composition (termed soret action). Many problems involving the flow of conductive physiological fluids, including blood and saline water, call for the study of the peristaltic transport of fluid in the presence of an external magnetic field and rotation [16]. We use a variety of values for the rotational parameters, the porous medium, density, amplitude wave,

and taper of the channel, as well as a variety of values for the Hartman number and Darcy number, to study the effects of varying the velocity and pressure gradient. The goal of this article is to investigate the rotation effects of the peristaltic transport of a Powell-Eyring fluid in an asymmetric channel through a porous medium subject to the combined actions of inclined MHD.

2. Problem Mathematical description

Consider how an incompressible Powell-Eyring fluid might move peristaltically in a two-dimensional, asymmetric conduit with a width of (d'+d). Flow is caused by an infinite sinusoidal wave moving with constant forward velocity (c) along the channel walls.
The geometry of the wall structure is described as:

$$\overline{h_1}(\bar{X},\bar{t}) = d - a_1 \sin\left[\frac{2\pi}{\lambda}(\bar{x}-c\bar{t})\right] \quad (1)$$

$$\overline{h_2}(\bar{X},\bar{t}) = -d' - a_2 \sin\left[\frac{2\pi}{\lambda}(\bar{x}-c\bar{t})+\Phi\right] \quad (2)$$

In which $\overline{h_1}(\bar{x},\bar{t})$ and $\overline{h_2}(\bar{x},\bar{t})$ are the lower and the upper walls, respectively. (d,d') denotes the channel width, (a_1,a_2) are the amplitudes of the wave,(λ) is the wavelength, (c) is the wave speed, (Φ) varies in the range $(0 \le \Phi \le \pi)$, when $\Phi = 0$ is a symmetric channel with out-of-phase waves and $\Phi = \pi$ waves are in phase, the rectangular coordinate system is chosen so that the $\bar{X} - axis$ is in the direction of the wave's motion. and the $\bar{Y} - axis$ perpendicular to $\bar{X}$, where $\bar{t}$ is the time.
Further, a_1, a_2, d, d' and Φ fulfill the following condition;

$$a_1^2 + a_2^2 + 2a_1a_2\cos\Phi \le (d+d')^2 \quad (3)$$

The Cauchy stress tensor $\bar{\tau}$ for a fluid that obeys the Powell- Eyring model is given as follows:-

$$\bar{\tau} = -\mathrm{PI} + \bar{\mathrm{S}} \quad (4)$$

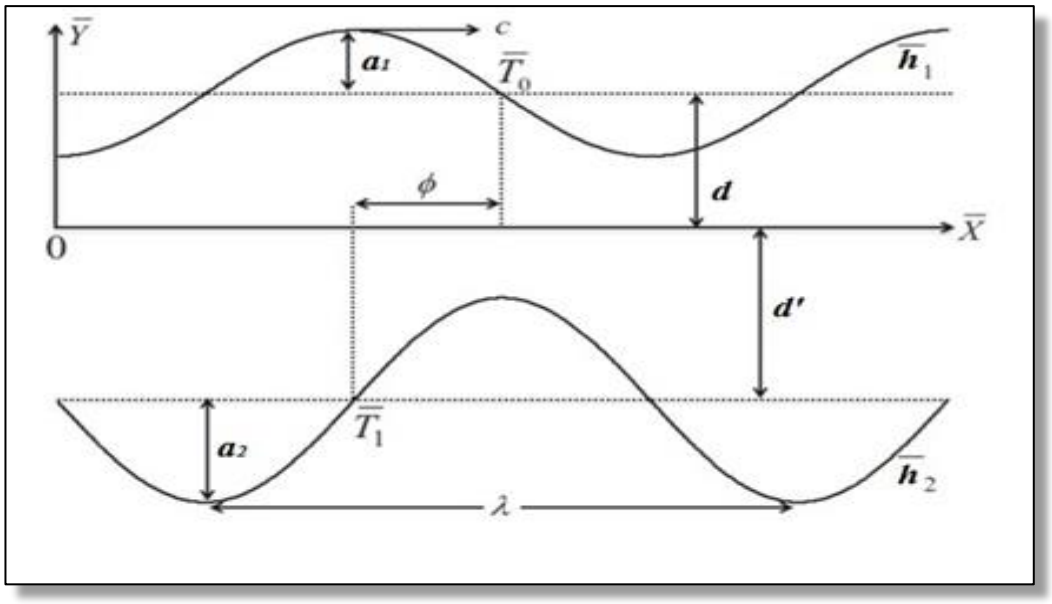

Figure 1: Coordinates for Asymmetric Channels in Cartesian Space

$$\bar{S} = \left[\mu + \frac{1}{\beta\gamma}\sinh^{-1}\left(\frac{\dot{\gamma}}{c_1}\right)\right] A_{11} \quad (5)$$

$$\dot{\gamma} = \sqrt{\frac{1}{2}\text{tras}(A_{11})^2} \quad (6)$$

$$A_{11} = \nabla\bar{V} + (\nabla\bar{V})^T \quad (7)$$

Where $\bar{S}$ is the extra stress tensor, I is the identity tensor, $\nabla = (\partial\bar{X}, \partial\bar{Y}, 0)$ is the gradient vector, (β, c_1) are the material parameters of Powell-Eyring fluid, P is the fluid pressure, and μ the dynamic viscosity. The term $\sinh^{-1}$ is approximately equivalent to

$$\sinh^{-1}\left(\frac{\dot{\gamma}}{c_1}\right) = \frac{\dot{\gamma}}{c_1} - \frac{\dot{\gamma}^3}{6{c_1}^3} \quad , \left|\frac{\dot{\gamma}^5}{6{c_1}^5}\right| \ll 1 \quad (8)$$

The flow is governed by three coupled nonlinear partial differentials of continuity, momentum, and energy, which are expressed in a frame $(\bar{X}, \bar{Y})$ as

$$\frac{\partial\bar{U}}{\partial\bar{X}} + \frac{\partial\bar{V}}{\partial\bar{Y}} = 0 \quad (9)$$

$$\rho\left(\frac{\partial\bar{U}}{\partial\bar{t}} + \bar{U}\frac{\partial\bar{U}}{\partial\bar{X}} + \bar{V}\frac{\partial\bar{U}}{\partial\bar{Y}}\right) - \rho\Omega\left(\Omega\bar{U} + 2\frac{\partial\bar{V}}{\partial\bar{t}}\right) = -\frac{\partial\bar{P}}{\partial\bar{X}} + \frac{\partial\bar{S}_{\bar{X}\bar{X}}}{\partial\bar{X}} + \frac{\partial\bar{S}_{\bar{X}\bar{Y}}}{\partial\bar{Y}} - \sigma{\beta_0}^2 cos\beta(\bar{U}cos\beta - \bar{V}sin\beta) - \frac{\mu}{\bar{k}}\bar{U} \quad (10$$

$$\rho\left(\frac{\partial\bar{V}}{\partial\bar{t}} + \bar{U}\frac{\partial\bar{V}}{\partial\bar{X}} + \bar{V}\frac{\partial\bar{V}}{\partial\bar{Y}}\right) - \rho\Omega\left(\Omega\bar{U} + 2\frac{\partial\bar{V}}{\partial\bar{t}}\right) = -\frac{\partial\bar{P}}{\partial\bar{Y}} + \frac{\partial\bar{S}_{\bar{X}\bar{Y}}}{\partial\bar{X}} + \frac{\partial\bar{S}_{\bar{Y}\bar{Y}}}{\partial\bar{Y}} - \sigma{\beta_0}^2 sin\beta(\bar{U}cos\beta - \bar{V}sin\beta) - \frac{\mu}{\bar{k}}\bar{V} \quad (11)$$

Where ρ is the fluid density, $\bar{V} = [\bar{U}, \bar{V}]$ is the velocity vector, $\bar{P}$ is the hydrodynamic pressure, $\bar{S}_{\bar{X}\bar{X}}, \bar{S}_{\bar{X}\bar{Y}}, and\ \bar{S}_{\bar{Y}\bar{Y}}$ are the elements of the extra stress tensor $\bar{S}$, σ is the electrical conductivity, β_0 is the constant magnetic field, β is the inclination of the magnetic field, Ω is the rotation C_P is specific heat, k' is the thermal conductivity, $\bar{T}$ is a temperature, and μ refers to the viscosity.

Listed below are the components of the extra stress tensor of Powell – Eying as defined by Eq.(5)

$$\bar{S}_{\bar{X}\bar{X}} = 2\left(\mu + \frac{1}{\beta C_1}\right)\bar{U}_{\bar{X}} - \frac{1}{3\beta{C_1}^3}\left[2{\bar{U}_{\bar{X}}}^2 + (\bar{V}_{\bar{X}} + \bar{U}_{\bar{Y}})^2 + 2{\bar{V}_Y}^2\right]\bar{U}_{\bar{X}} \quad (12)$$

$$\bar{S}_{\bar{X}\bar{Y}} = 2\left(\mu + \frac{1}{\beta C_1}\right)(\bar{V}_{\bar{X}} + \bar{U}_{\bar{Y}}) - \frac{1}{6\beta{C_1}^3}\left[2{\bar{U}_{\bar{X}}}^2 + (\bar{V}_{\bar{X}} + \bar{U}_{\bar{Y}})^2 + 2{\bar{V}_Y}^2\right](\bar{V}_{\bar{X}} + \bar{U}_{\bar{Y}}) \quad (13)$$

$$\bar{S}_{\bar{Y}\bar{Y}} = 2\left(\mu + \frac{1}{\beta C_1}\right)\bar{V}_{\bar{Y}} - \frac{1}{3\beta{C_1}^3}\left[2{\bar{U}_{\bar{X}}}^2 + (\bar{V}_{\bar{X}} + \bar{U}_{\bar{Y}})^2 + 2{\bar{V}_Y}^2\right]\bar{V}_{\bar{Y}} \quad (14)$$

Natural peristaltic motion is an erratic occurrence, but by applying the transformation from laboratory frame, the stability can be assumed (fixed frame) $(\bar{X}, \bar{Y})$to wave frame (move frame) $(\bar{x}, \bar{y})$. The subsequent transformations determine the relationship between coordinates, velocities, and pressure in the laboratory frame $(\bar{X}, \bar{Y})$ to the wave frame $(\bar{x}, \bar{y})$

$$\bar{x} = \bar{X} - c, \bar{y} = \bar{Y}, \bar{u} = \bar{U} - c, \bar{v} = \bar{V}, \bar{p}(\bar{x}, \bar{y}) = \bar{P}(\bar{X}, \bar{Y}, \bar{t}) \quad (15)$$

Where $\bar{u}$ and $\bar{v}$ represent the velocity factors and $\bar{p}$ represents the pressure in the wave frame. We now substitute equation (15) in equations (1), (2), and (9-14) and normalize the resulting equation with the following non-dimensional variables:

$$x = \frac{1}{\lambda}\bar{x},\ y = \frac{1}{d}\bar{y}\ u = \frac{1}{c}\bar{U},\ v = \frac{1}{\delta c}\bar{V},\ P = \frac{d^2}{\lambda\,\mu\,c}\bar{P},\ t = \frac{c}{\lambda}\bar{t},\ h_1 = \frac{1}{d}\overline{h_1},\ h_2 = \frac{1}{d}\overline{h_2},$$
$$\delta = \frac{d}{\lambda},\ Re = \frac{\rho\,c\,d}{\mu},\ Ha = d\sqrt{\frac{\bar{\sigma}}{\mu}}\beta_0,\ Da = \frac{\bar{k}}{d^2},\ w = \frac{1}{\mu\,\beta\,C_1},\ A = \frac{w}{6}\left(\frac{C}{C_1\,d}\right)^2,\ \bar{T} = T - \quad (16)$$
$$T_0,\ \theta = \frac{T-T_0}{T_1-T_0},\ S_{xx} = \frac{\lambda}{\mu\,c}\bar{S}_{\bar{X}\bar{X}},\ S_{xy} = \frac{d}{\mu\,c}\bar{S}_{\bar{X}\bar{Y}},\ S_{yy} = \frac{d}{\mu\,c}\bar{S}_{\bar{Y}\bar{Y}}$$

Where, (δ) is the wave number, $(h_1)\ and\ (h_2)$ are non-dimensional lower and upper wall surfaces, respectively. (Re) is the Reynolds number, (Ha) is the Hartman number, (Φ) is the amplitude ratio, (w) is the non-dimensional permeability of the porous medium parameter, (Da) is the Darcy number, (A) is the Powell-Eyring fluid parameter, $(T_0)\ and\ (T_1)$ are the temperatures at the upper and lower walls.

Next, we have

$$h_1(x,t) = 1 - a\sin(2\pi x) \quad (17)$$
$$h_2(x,t) = -d^* - b\ sin\ (2\pi x + \Phi) \quad (18)$$

We have where a, b, d^* and Φ satisfy equation (3)

$$a^2 + b^2 + 2ab\cos\Phi \le (1+d^*)^2 \quad (19)$$
$$\frac{\partial u}{\partial x} + \frac{\partial v}{\partial y} = 0 \quad (20)$$

$$Re\delta\left(\frac{\partial u}{\partial t} + u\frac{\partial u}{\partial x} + v\frac{\partial u}{\partial y}\right) - \frac{\rho d^2\Omega}{\mu}\left(\Omega u + 2\frac{\delta c}{d}\frac{\partial v}{\partial t}\right) = -\frac{\partial p}{\partial x} + \delta^2\frac{\partial}{\partial x}S_{xx} + \frac{\partial}{\partial y}S_{xy} - \quad (21)$$
$$Ha^2\cos\beta\ (u\cos\beta - \delta v\sin\beta) - \frac{1}{Da}u$$

$$Re\delta^3\left(\frac{\partial v}{\partial t} + u\frac{\partial v}{\partial x} + v\frac{\partial v}{\partial y}\right) - \frac{\rho d^2\Omega\delta}{\mu}\left(\Omega u + 2\frac{\delta c}{d}\frac{\partial v}{\partial t}\right) = -\frac{\partial p}{\partial x} + \delta^2\ \frac{\partial}{\partial x}S_{xy} + \quad (22)$$
$$\delta\frac{\partial}{\partial y}S_{yy} + Ha^2\sin\beta\ (\delta u\cos\beta - \delta^2 v\sin\beta) - \delta^2\frac{1}{Da}\ v$$

$$S_{xx} = 2(1+w)\frac{\partial u}{\partial x} - 2A\left[2\delta^2\left(\frac{\partial u}{\partial x}\right)^2 + \left(\frac{\partial u}{\partial y} + \delta^2\frac{\partial v}{\partial x}\right)^2 + 2\delta^2\left(\frac{\partial v}{\partial y}\right)^2\right]\frac{\partial u}{\partial x} \quad (23)$$

$$S_{xy} = (1+w)\left(\delta^2\frac{\partial v}{\partial x} + \frac{\partial u}{\partial y}\right) - A\left[2\delta^2\left(\frac{\partial u}{\partial x}\right)^2 + \left(\frac{\partial u}{\partial y} + \delta^2\frac{\partial v}{\partial x}\right)^2 + \right. \quad (24)$$
$$\left. 2\delta^2\left(\frac{\partial v}{\partial y}\right)^2\right]\left(\delta^2\frac{\partial v}{\partial x} + \frac{\partial u}{\partial y}\right)$$

$$S_{yy} = 2(1+w)\delta\frac{\partial v}{\partial y} - 2A\delta\left[2\delta^2\left(\frac{\partial u}{\partial x}\right)^2 + \left(\frac{\partial u}{\partial y} + \delta^2\frac{\partial v}{\partial x}\right)^2 + 2\delta^2\left(\frac{\partial v}{\partial y}\right)^2\right]\frac{\partial v}{\partial y} \quad (25)$$

In previous equations, Pr is the Prandtl number, Ec is the Eckert number and θ is the dimensionless temperature.

Following are the relations between the stream function (ψ) and velocity components:

$$u = \frac{\partial\Psi}{\partial y},\ v = -\frac{\partial\Psi}{\partial x} \quad (26)$$

Substituting equation (26) into equations (21) to (25), noting that the mass balance displayed by equation (20) is similarly satisfied, this produces the consequence that equation (26) is satisfied.

$$Re\ \delta\left(\frac{\partial^2\Psi}{\partial t\partial y} + \frac{\partial^3\Psi}{\partial x\partial y^2} - \frac{\partial^3\Psi}{\partial x\partial y^2}\right) - \frac{\rho d^2\Omega}{\mu}\left(\Omega\frac{\partial\Psi}{\partial y} - 2\frac{\delta c}{d}\ \frac{\partial^2\Psi}{\partial t\partial x}\right) = -\frac{\partial \mathrm{p}}{\partial x} + \quad (27)$$
$$\delta^2\frac{\partial}{\partial x}\ S_{xx} + \frac{\partial}{\partial y}S_{xy} - Ha^2\cos\beta\left(\frac{\partial\Psi}{\partial y}\ \cos\beta + \delta\frac{\partial\Psi}{\partial x}\sin\beta\right) - \frac{1}{Da}\frac{\partial\Psi}{\partial y}$$

$$Re\ \delta^3\left(-\frac{\partial^2\Psi}{\partial t\partial x} - \frac{\partial^3\Psi}{\partial x^2\partial y} - \frac{\partial^3\Psi}{\partial x^2\partial y}\right) - \frac{\rho d^2\Omega\delta}{\mu}\left(\Omega\frac{\partial\Psi}{\partial x} - 2\frac{\delta c}{d}\ \frac{\partial^2\Psi}{\partial t\partial x}\right) = -\frac{\partial \mathrm{p}}{\partial y} + \quad (28)$$
$$\delta^2\frac{\partial}{\partial x}\ S_{xy} + \delta\frac{\partial}{\partial y}S_{yy} + Ha^2\sin\beta\left(\delta\frac{\partial\Psi}{\partial y}\ \cos\beta + \delta^2\frac{\partial\Psi}{\partial x}\sin\beta\right) + \delta^2\frac{1}{Da}\frac{\partial\Psi}{\partial x}$$

$$S_{xx} = 2(1+w)\frac{\partial^2\Psi}{\partial x\partial y} - 2A\left[2\delta^2\left(\frac{\partial^2\Psi}{\partial x\partial y}\right)^2 + \left(\frac{\partial^2\Psi}{\partial y^2} - \delta^2\frac{\partial^2\Psi}{\partial x^2}\right)^2 + 2\delta^2\left(\frac{\partial^2\Psi}{\partial x\partial y}\right)^2\right] \quad (29)$$

$$S_{xy} = (1+w)\left(-\delta^2\frac{\partial^2\Psi}{\partial x^2} + \frac{\partial^2\Psi}{\partial y^2}\right) - A\left[2\delta^2\left(\frac{\partial^2\Psi}{\partial x\partial y}\right)^2 + \left(-\delta^2\frac{\partial^2\Psi}{\partial x^2} + \delta^2\frac{\partial\Psi}{\partial y^2}\right)^2 + 2\delta^2\left(-\frac{\partial^2\Psi}{\partial x\partial y}\right)^2\right]\left(-\delta^2\frac{\partial^2\Psi}{\partial x^2} + \frac{\partial^2\Psi}{\partial y^2}\right) \quad (30)$$

$$S_{yy} = -2(1+w)\delta\frac{\partial^2\Psi}{\partial x\partial y} - 2A\delta\left[2\delta^2\left(\frac{\partial^2\Psi}{\partial x\partial y}\right)^2 + \left(\frac{\partial^2\Psi}{\partial y^2} - \delta^2\frac{\partial^2\Psi}{\partial x^2}\right)^2 + 2\delta^2\left(\frac{\partial^2\Psi}{\partial x\partial y}\right)^2\right]\left(-\frac{\partial^2\Psi}{\partial x\partial y}\right) \quad (31)$$

Now, the equations from (27) to (31) become the form when $(Re\ and\ \ \delta \ll 1)$ are present:

$$-\frac{\rho d^2\Omega^2}{\mu}\frac{\partial\Psi}{\partial y} = -\frac{\partial \mathrm{p}}{\partial x} + \frac{\partial}{\partial y}S_{xy} - \left(Ha^2\cos^2\beta + \frac{1}{Da}\right)\frac{\partial\Psi}{\partial y} \quad (32)$$

$$-\frac{\partial \mathrm{p}}{\partial y} = 0 \quad (33)$$

While the component of the extra stress tensor becomes the form of

$$S_{xx} = 2(1+w)\frac{\partial^2\Psi}{\partial x\partial y} - 2A\left(\frac{\partial^2\Psi}{\partial y^2}\right)^2\frac{\partial^2\Psi}{\partial x\partial y} \quad (34)$$

$$S_{xy} = (1+w)\left(\frac{\partial^2\Psi}{\partial y^2}\right) - A\left(\frac{\partial^2\Psi}{\partial y^2}\right)^3 \quad (35)$$

$$S_{yy} = 0 \quad (36)$$

Also, if equation (35) is entered into equation (32) as well as the derivative regards to y and by (w+1) is taken, then the following equation is obtained:

$$\frac{\partial^4\Psi}{\partial y^4} - \eta A\frac{\partial^2}{\partial y^2}\left(\frac{\partial^2\Psi}{\partial y^2}\right)^3 - \zeta\frac{\partial^2\Psi}{\partial y^2} = 0 \quad (37)$$

Where

$$\zeta = \frac{Ha^2\cos^2\beta + \frac{1}{Da} - \frac{\rho d^2\Omega^2}{\mu}}{w+1},\ \eta = \frac{1}{w+1}$$

In the wave frame, the dimensionless volume flow rate and boundary condition are as follows:

$$\Psi = \frac{F}{2}\ ,\frac{\partial\Psi}{\partial y} = -1\ ,\theta = 0 \quad at \quad y = h_1 \quad (38)$$

$$\Psi = -\frac{F}{2}\ ,\frac{\partial\Psi}{\partial y} = -1\ ,\theta = 0 \quad at\ \ y = h_2 \quad (39)$$

F represents the dimensionless temporal average flow in the wave frame.

3. Problem's Resolution

The perturbation method is used to obtain the solution of a non-linear partial differential equation system by increasing flow amounts in a power series of A.

$$\Psi = \Psi_0 + A\Psi_1 + O(A^2) \quad (40)$$

$$P = P_0 + AP_1 + O(A^2) \quad (41)$$

Now, by substituting Equations (40) - (41) into Equations (32) - (37) and boundary conditions (38) - (39) and comparing the coefficients of the same A power up to the first order yields the two system solutions listed below:

3.1. Zeroth order system

When the terms of order (A) in a zeroth-order system are negligible, we obtain

$$\Psi_{0yyyy} - \zeta\Psi_{0yy} = 0 \quad (42)$$

Such is the case

$$\Psi_0 = \frac{F_0}{2}\ ,\frac{\partial\Psi_0}{\partial y} = -1 \quad at\ \ y = h_1 \quad (43)$$

and

$$\Psi_0 = -\frac{\mathrm{F}_0}{2}, \frac{\partial \Psi_0}{\partial y} = -1 \quad at \quad y = h_2 \tag{44}$$

3.2. First order system

$$\Psi_{1yyyy} - \eta \frac{\partial^2}{\partial y^2}\left(\Psi_{0yy}\right)^3 - \zeta \Psi_{1yy} = 0 \tag{45}$$

$$\Psi_{1yyyy} - \zeta \Psi_{1yy} = \eta \frac{\partial^2}{\partial y^2}\left(\Psi_{0yy}\right)^3 \tag{46}$$

$$\Psi_1 = \frac{\mathrm{F}_1}{2}, \ \frac{\partial \Psi_1}{\partial y} = 0 \ \ at \ \ y = h_1 \tag{27}$$

and

$$\Psi_1 = -\frac{\mathrm{F}_1}{2}, \ \frac{\partial \Psi_1}{\partial y} = 0 \ \ at \ \ y = h_2 \tag{48}$$

Solving associated zeroth and first-order systems yields the final equation for the stream function.

$$\Psi = \Psi_0 + \mathrm{A}\Psi_1 \tag{49}$$

$$\begin{aligned}\Psi = {} & \frac{e^{-y\sqrt{\zeta}}\left(e^{2y\sqrt{\zeta}}\mathrm{c1}+\mathrm{c2}\right)}{\zeta} + \mathrm{c3} + y\mathrm{c4} + \mathrm{A}[(e^{-3y\sqrt{\zeta}}(e^{3(\mathrm{h1}+\mathrm{h2})\sqrt{\zeta}}(\mathrm{F0}+\mathrm{h1}-\mathrm{h2})^3\zeta^3\eta - \\ & e^{6y\sqrt{\zeta}}(\mathrm{F0}+\mathrm{h1}-\mathrm{h2})^3\zeta^3\eta + 6e^{(\mathrm{h1}+\mathrm{h2}+4y)\sqrt{\zeta}}(\mathrm{F0}+\mathrm{h1}-\mathrm{h2})^3(-5+2y\sqrt{\zeta})\zeta^3\eta + \\ & 6e^{2(\mathrm{h1}+\mathrm{h2}+y)\sqrt{\zeta}}(\mathrm{F0}+\mathrm{h1}-\mathrm{h2})^3(5+2y\sqrt{\zeta})\zeta^3\eta + 8e^{(3\mathrm{h1}+4y)\sqrt{\zeta}}(-2+\mathrm{h1}\sqrt{\zeta} - \\ & \mathrm{h2}\sqrt{\zeta})^3\mathrm{A1} + 24e^{(\mathrm{h1}+2\mathrm{h2}+4y)\sqrt{\zeta}}(-2+\mathrm{h1}\sqrt{\zeta}-\mathrm{h2}\sqrt{\zeta})(2+\mathrm{h1}\sqrt{\zeta}-\mathrm{h2}\sqrt{\zeta})^2\mathrm{A1} - \\ & 8e^{(3\mathrm{h2}+4y)\sqrt{\zeta}}(-2-\mathrm{h1}\sqrt{\zeta}+\mathrm{h2}\sqrt{\zeta})^3\mathrm{A1} + 24e^{(2\mathrm{h1}+\mathrm{h2}+4y)\sqrt{\zeta}}(2+\mathrm{h1}\sqrt{\zeta} - \\ & \mathrm{h2}\sqrt{\zeta})(2-\mathrm{h1}\sqrt{\zeta}+\mathrm{h2}\sqrt{\zeta})^2\mathrm{A1} + 8e^{(3\mathrm{h1}+2y)\sqrt{\zeta}}(-2+\mathrm{h1}\sqrt{\zeta}-\mathrm{h2}\sqrt{\zeta})^3\mathrm{A2} + \\ & 24e^{(\mathrm{h1}+2(\mathrm{h2}+y))\sqrt{\zeta}}(-2+\mathrm{h1}\sqrt{\zeta}-\mathrm{h2}\sqrt{\zeta})(2+\mathrm{h1}\sqrt{\zeta}-\mathrm{h2}\sqrt{\zeta})^2\mathrm{A2} - \\ & 8e^{(3\mathrm{h2}+2y)\sqrt{\zeta}}(-2-\mathrm{h1}\sqrt{\zeta}+\mathrm{h2}\sqrt{\zeta})^3\mathrm{A2} + 24e^{(2\mathrm{h1}+\mathrm{h2}+2y)\sqrt{\zeta}}(2+\mathrm{h1}\sqrt{\zeta} - \\ & \mathrm{h2}\sqrt{\zeta})(2-\mathrm{h1}\sqrt{\zeta}+\mathrm{h2}\sqrt{\zeta})^2\mathrm{A2}))/(8(e^{\mathrm{h1}\sqrt{\zeta}}(-2+\mathrm{h1}\sqrt{\zeta}-\mathrm{h2}\sqrt{\zeta}) + e^{\mathrm{h2}\sqrt{\zeta}}(2 + \\ & \mathrm{h1}\sqrt{\zeta}-\mathrm{h2}\sqrt{\zeta}))^3\zeta) + \mathrm{A3} + y\mathrm{A4}]\end{aligned} \tag{50}$$

Within the fixed frame, the axial velocity component is expressed as follows:

$u(x, y, t) = \Psi_{\mathrm{y}}$

It is possible to rewrite (37) as

$$\frac{\partial p}{\partial x} = \Psi_{0yyy} - \zeta \Psi_{0y} + A\Psi_{1yyy} - \eta A \frac{\partial}{\partial y}\left(\Psi_{0yy}\right)^3 - A\zeta\Psi_{1y}$$

4. Results and discussions

This section consists of two subsections. In the first one, the velocity distribution is discussed, while in the second subsection, the pressure gradient is illustrated using the MATHEMATICA software.

I. Velocity distribution u:

The axial velocity across the channel is varied as it is indicated by the case variation of u. The effect of different values (Ha, Da, w, A, a, b, and d) on the axial velocity u is shown in Figures. (2) – (11), where the behavior of the velocity distribution is parabolic as shown in the following figures:

1- Figures (2) and (8) demonstrate that axial velocity falls with increasing Hartman number (Ha) and material fluid parameter (A) in the channel's central region, while it increases at the channel's wall.

2- Figures (3),(4),(5),(6), and (11) demonstrated that the axial velocity increases as the Darcy number (Da), inclination of magnetic field (β), rotation (Ω), porous medium parameter (w), and

width of the channel (d) increase within the middle of the channel, but decreases at the channel wall boundary.

3- Figure (7) demonstrates that for approximately 0.05<y<0.9, the axial velocity decreases as the amplitude ratio (ϕ) increases, whereas otherwise, it increases.

4- Figure (9) demonstrates that for -0.4<y<0.55, the axial velocity increases as the wave amplitude increases (a) and decreases with increasing wave amplitude (a) for all other values of y.

5- Figure (10) demonstrates that for -0.05<y<0.85, the axial velocity increases as the wave amplitude increases (b), but decreases with decreasing wave amplitude (b).

II. Pressure gradient dp/dx:

The effect of relevant parameters on the pressure gradient dp/dx is graphically illustrated in Figures. (12)-(21)

1- In Figures (12), (18), and (19), the increase in the values of Hartman number (Ha), material fluid parameter (A), and amplitude of the wave (a) give rise to the axial pressure gradient decreases as the vertex of the curve is twisted to the right but there is no effect on axial pressure gradient near the right or left wall of the channel.

2-In Figures (13),(14), and (16), the increase in the values of Darcy number (Da), the inclination of magnetic field (β), and the porous medium parameter (w) lead to the axial pressure gradient increases as the vertex of the curve is twisted to the right but there is no effect on the axial pressure gradient near the channel's right or left walls.

3-Figure (20) increases in the amplitude of the wave (b) decreases the axial pressure gradient as the curve's vertex is twisted to the left, but there is no effect on the axial pressure gradient near the channel's right or left walls.

4-Figures (15) and (21) demonstrate that the axial pressure gradient does not change as the rotation (Ω) and channel width (d) values increase.

5- Figure (17) for approximately -2.75<x<-4 , the axial velocity increases as the amplitude ratio increases (ϕ) , for approximately -1.75<x<-2.75, the axial pressure gradient increases slightly, and for 0<x<-1.75, the axial pressure gradient increases. However, for x>0, the axial pressure gradient does not.

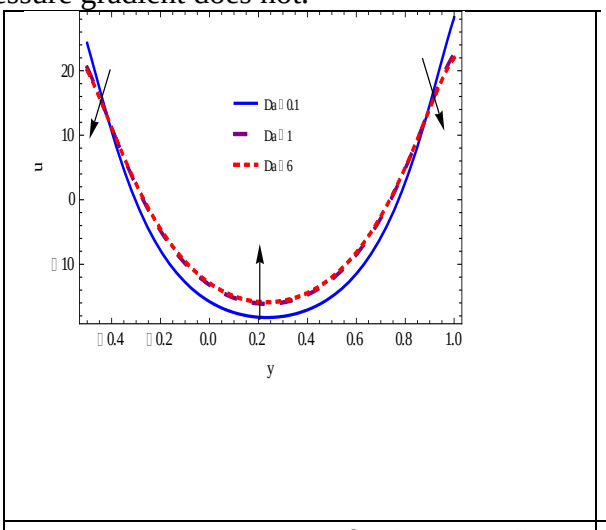

Figure 2: Variation of velocity with respect to (Da) values when β=0.1, Da $= 6, \rho = 0.1, d = 0.5, \Omega = 0.3, \mu = 3, w = 0.3, \phi = 0.5, a = 0.2,$ $b = 0.2, d_1 = 0.5, \mathrm{F0} = 0.4, \mathrm{F1} = 0, A = 5$

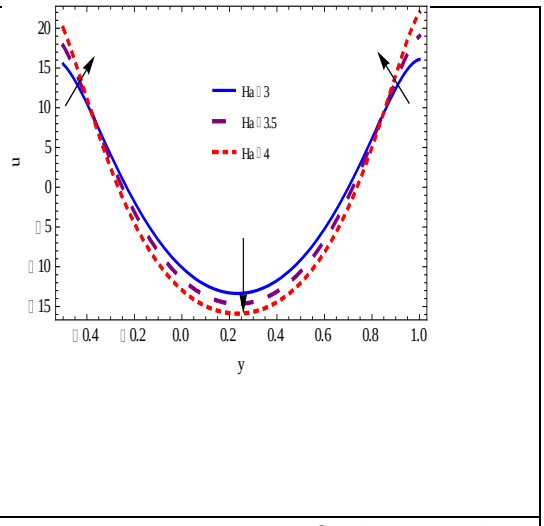

Figure 3: Variation of velocity with respect to (Ha) values when Ha= 4, β = 0.1, Da $= 6, \rho = 0.1, d = 0.5 \Omega = 0.3, \mu = 3, w = 0.3, \phi = 0.5,$ $a = 0.2, b = 0.2, d_1 = 0.5, \mathrm{F0} = 0.4, \mathrm{F1} = 0, A = 5$

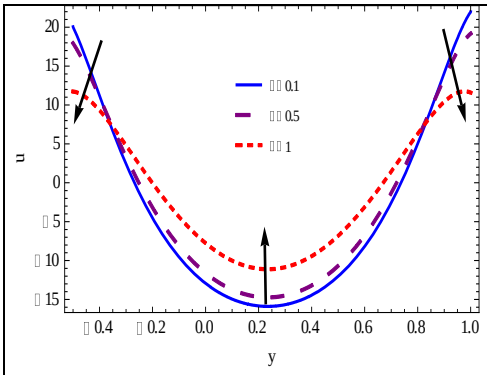

Figure 4: Variation of velocity with respect to(β) values when Ha=4,Da = $6, \rho = 0.1, d = 0.5$ $, \Omega = 0.3, \mu = 3\ , w = 0.3, \phi = 0.5, a = 0.2,$ $b = 0.2, d_1 = .5, \mathrm{F0} = 0.4, \mathrm{F1} = 0, A = 5$

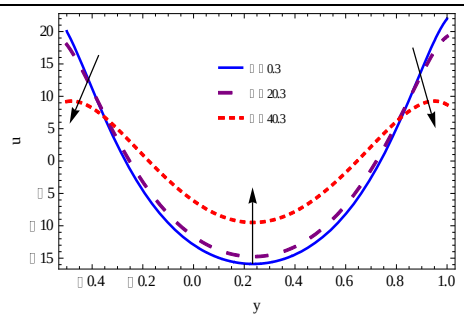

Figure 5: Variation of velocity with respect to(Ω) values when Ha= $4, \beta = 0.1, \mathrm{Da} = 6, \rho = 0.1,$ $d = 0.5, \mu = 3, w = 0.3, \phi = 0.5, a = 0.2,$ $b = 0.2, d_1 = 0.5, \mathrm{F0} = 0.4, \mathrm{F1} = 0, A = 5$

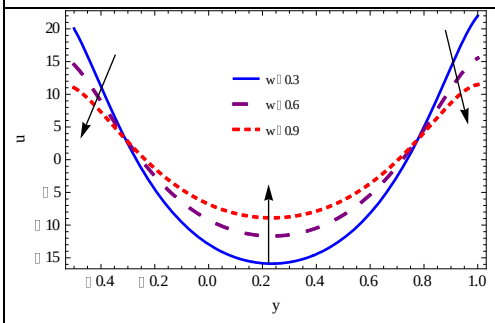

Figure 6: Variation of velocity with respect to(w) values when Ha= 4, $\beta = 0.1, \mathrm{Da} = 6, \rho = 0.1,$ $d = 0.5, \quad \Omega = 0.3, \mu = 3, , \phi = 0.5, a = 0.2,$ $b = 0.2, \ d_1 = 0.5, \mathrm{F0} = 0.4, \mathrm{F1} = 0, \ A = 5$

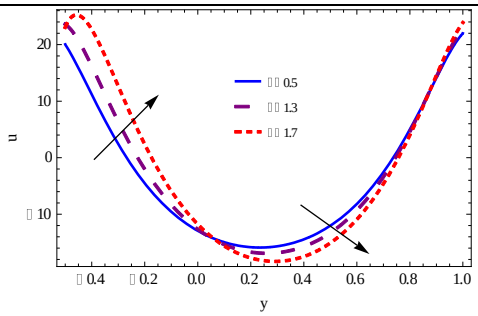

Figure 7: Variation of velocity with respect to(ϕ) values when Ha= 4, $\beta = 0.1, \mathrm{Da} = 6, \rho = 0.1,$ $d = 0.5, \quad \Omega = 0.3, \mu = 3, , w = 0.3, a = 0.2,$ $b = 0.2, \quad d_1 = 0.5, \mathrm{F0} = 0.4, \mathrm{F1} = 0,$ $A = 5$

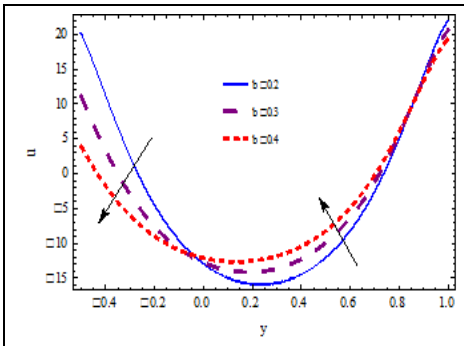

Figure 8: Variation of velocity with respect to(A) values when Ha= 4, $\beta = 0.1, \mathrm{Da} = 6, \rho = 0.1, d = 0.5, \Omega = 0.3, w = 0.3, \phi = 0.5, a = 0.2, , \mu = 3, b = 0.2, \mathrm{F0} = 0.4, \mathrm{F1} = 0$

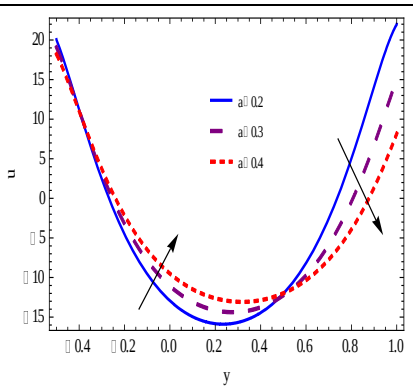

Figure 9: Variation of velocity with respect to(a) values when Ha= 4, β = 0.1, Da=6, ρ=0.1, d=0.5, Ω=0.3, w=0.3, ϕ=0.5, μ=3, b=0.2, F0=0.4, F1=0, A=5

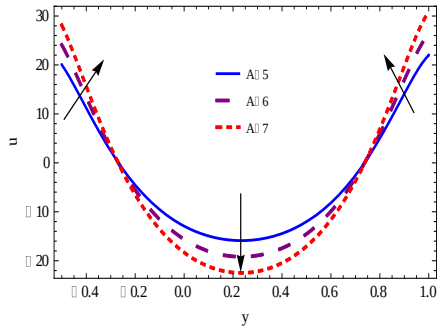

Figure 10: Variation of velocity with respect to (b) values when Ha= 4, β = 0.1, Da=6, ρ=0.1, d=0.5, Ω=0.3, w=0.3, ϕ=0.5, a=0.2, μ=3, F0=0.4, F1=0, A=5

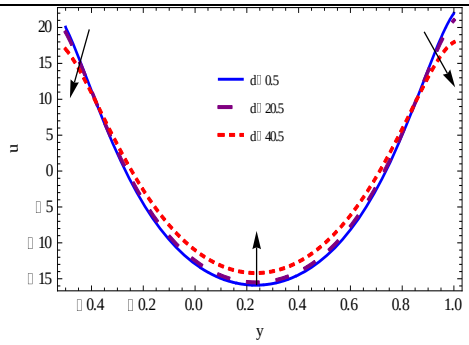

Figure 11: Variation of velocity with respect to (d) values when Ha= 4, β = 0.1, Da=6, ρ=0.1, Ω =0.3, w=0.3, ϕ=0.5, a=0.2, μ=3, b=0.2, F0=0.4, F1=0, A=5

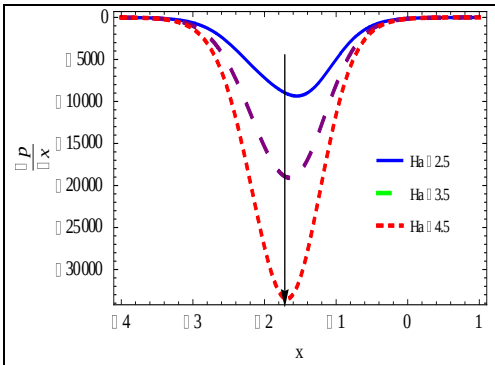

Figure12: Variation in pressure gradient for various values of (Ha) when $\beta = 0.1, \mathrm{Da} = 0.2, \rho = 0.1, d = 0.5, \Omega = 0.2, \mu = 3, w = 0.3, \phi = 0.2, a = 0.2, b = 0.2, d_1 = 0.5, \mathrm{F0} = 0.4, \mathrm{F1} = 0, A = 0.3$

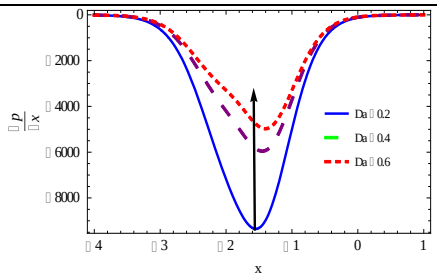

Figure 13: Variation in pressure gradient for various values of (Da) when $\mathrm{Ha} = 2.5, \beta = 0.1, \rho = 0.1, d = 0.5, \Omega = 0.2, \mu = 3, w = 0.3, \phi = 0.2, a = 0.2, b = 0.2, d_1 = 0.5, \mathrm{F0} = 0.4, \mathrm{F1} = 0, A = 0.3$

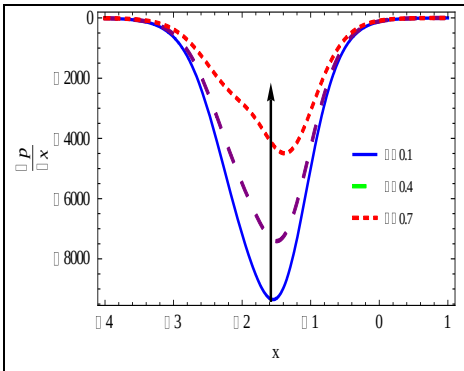

Figure14: Variation in pressure gradient for various values of (β) when Ha =2.5, Da $= 0.2, \rho = 0.1$ $, d = 0.5, \Omega = 0.2,\ \mu = 3, w = 0.3,\ \phi =$ .2, $a = 0.2, b = 0.2, d_1 = 0.5, \mathrm{F0} =$ $0.4, \mathrm{F1} = 0$ $, A = 0.3$

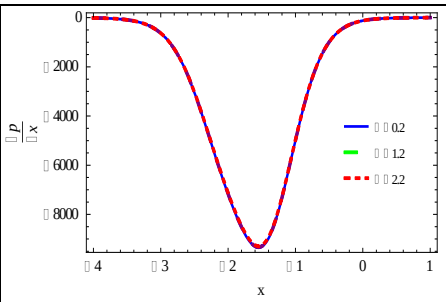

Figure15: Variation in pressure gradient for various values of (Ω) when Ha= 2.5, $\beta = 0.1, \mathrm{Da} = 0.2,$ $\rho = 0.1, a = 0.2,\ \ d = 0.5,\ \mu = 3, w =$ 0.3, $\phi = 0.2,\ b = 0.2, d_1 = 0.5, \mathrm{F0} =$ $0.4, \mathrm{F1} = 0, A = 0.3$

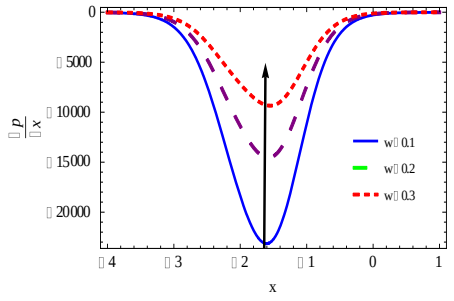

Figure16: Variation in pressure gradient for various values of (w) when Ha= 2.5, $\beta = 0.1, \mathrm{Da} = 0.2,$ $\rho = 0.1, d = 0.5, \Omega = 0.2, \mu = 3, \phi =$ 0.5, $a = 0.2, b = 0.2, d_1 = 0.5, \mathrm{F0} =$ $0.4, \mathrm{F1} = 0, A = 0.3$

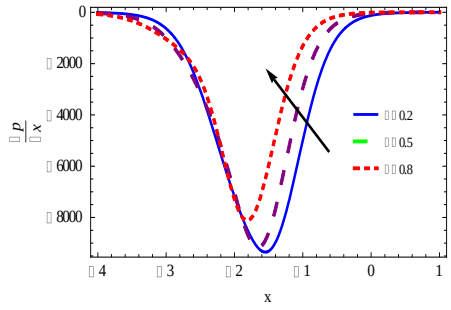

Figure17: Variation in pressure gradient for various values of (ϕ) when Ha= 2.5, $\beta = 0.1, \mathrm{Da} = 0.2,$ $\rho = 0.1,\ \ d = 0.5, \Omega = 0.2, \mu = 3, w =$ 0.3, $a = 0.2, b = 0.2, d_1 = 0.5, \mathrm{F0} =$ $0.4, \mathrm{F1} = 0, A = 0.3$

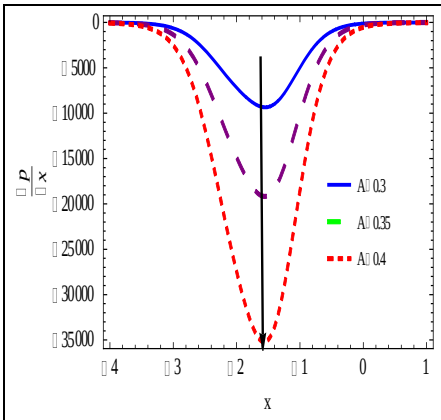

Figure18: Variation in pressure gradient various values of (A) when Ha= 2.5, $\beta = 0.1, \mathrm{Da} = 0.2,$ $\rho = 0.1, d = 0.5, \Omega = 0.2, \mu = 3, w = 0.3,$ $\phi = 0.5, a = 0.2, b = 0.2, d_1 = 0.5, \mathrm{F0} = 0.4,$ $\mathrm{F1} = 0$

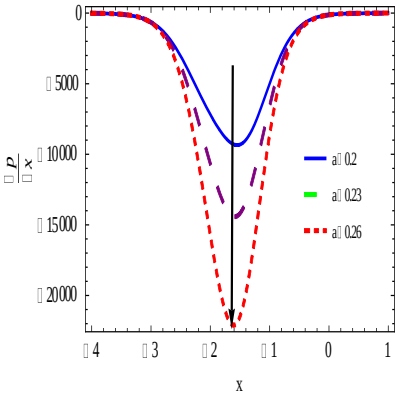

Figure19: Variation in pressure gradient various values of (a) when Ha= 2.5, $\beta = 0.1, \mathrm{Da} = 0.2,$ $\rho = 0.1, d = 0.5, \Omega = 0.2, \mu = 3, w = 0.3,$ $\phi = 0.5, b = 0.2, d_1 = 0.5, \mathrm{F0} = 0.4, \mathrm{F1} = 0.4$ $, A = 0.3$

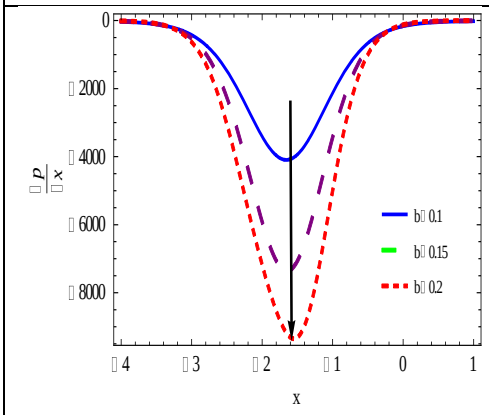

Figure 20: Variation in pressure gradient various values of (b) when Ha= 2.5, $\beta = 0.1, \mathrm{Da} = 0.2,$ $\rho = 0.1, d = 0.5, \Omega = 0.2, \mu = 3, w = 0.3,$ $\phi = 0.5, a = 0.2, d_1 = 0.5, \mathrm{F0} = 0.4, \mathrm{F1} = 0.4$ $, A = 0.3$

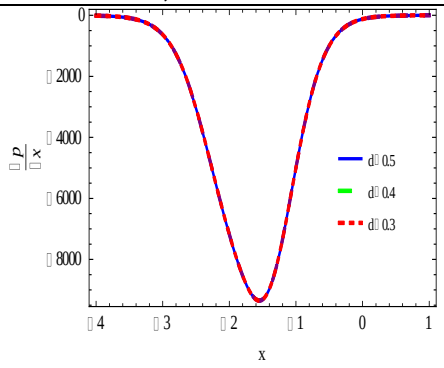

Figure 21: Variation in pressure gradient various values of (d) when Ha= 2.5, $\beta = 0.1, \mathrm{Da} = 0.2,$ $\rho = 0.1, \Omega = 0.2, \mu = 3, w = 0.3,$ $\phi = 0.5,$ $a = 0.2, b = 0.2, d_1 = 0.5, \mathrm{F0} = 0.4, \mathrm{F1} = 0.4$ $, A = 0.3$

5. Conclusion

In this study, the rotational effects of peristaltic transport of a Powell-Eyring fluid in an asymmetric channel through a porous material susceptible to the combined acts of inclined MHD are investigated. The asymmetric channel is formed by selecting peristaltic waves with varying amplitudes and phases on the non-uniform walls and a low Reynolds number. Using the perturbation approach, the formulas for the axial velocity and pressure gradient are produced. Multiple graphs are utilized for parameter analysis.

I) With increasing Hartman number (Ha) and material fluid parameter (A), in the middle of the channel, the axial velocity falls, while the axial velocity increases at the channel wall boundary. However, the opposite occurs for increasing the Darcy number (Da), the inclination of the magnetic field (β), the rotation (Ω), the porous medium parameter (w), and the width of the channel (d). The axial velocity decreases at the channel wall boundary, while for about $0.05<y<0.9$ of the axial velocity decreases as the amplitude ratio (ϕ) increases, and it increases otherwise, for approximately $-0.4<y<0.55$, the axial velocity increases as the wave amplitude increases (a) and decreases when the amplitude of the wave (a) increases, and for approximately $-0.05<y<0.85$, the axial velocity increases as the wave amplitude increases (b), but it decreases when the amplitude of the wave (b) increases.

II) When the values of Hartman number (Ha), material fluid parameter (A), and amplitude of the wave (a) increase, the axial pressure gradient decreases as the vertex of the curve is twisted to the right. However, there is no effect on the axial pressure gradient near the channel's right or left walls. However, the opposite occurs when the values of Darcy number (Da), the inclination of magnetic field (β), and porous medium parameter (w) increase whereas increases in the amplitude of the wave (b) cause the axial pressure gradient to decrease as the vertex of the curve is twisted to the left, neither there is no effect on the axial pressure gradient near the channel's right or left walls, nor it does the axial pressure gradient change as the value of the rotation (Ω) increases.

References

[1] T. W. Latham, "Fluid motion in peristaltic pumps, M S." Thesis, MIT, Cambridge, MA, 1966.

[2] S. Hina, M. Mustafa, T. Hayat, and A. Alsaedi, "Peristaltic flow of Powell-Eyring fluid in curved channel with heat transfer: A useful application in biomedicine," *Comput. Methods Programs Biomed.*, vol. 135, pp. 89–100, 2016.

[3] T. Hayat, N. Aslam, M. Rafiq, and F. E. Alsaadi, "Hall and Joule heating effects on peristaltic flow of Powell–Eyring liquid in an inclined symmetric channel," *Results Phys.*, vol. 7, pp. 518–528, 2017.

[4] H. A. Ali and A. M. Abdulhadi, "Analysis of Heat Transfer on Peristaltic Transport of Powell-Eyring Fluid in an Inclined Tapered Symmetric Channel with Hall and Ohm's Heating Influences," *J. AL-Qadisiyah Comput. Sci. Math.*, vol. 10, no. 2, p. Page-26, 2018.

[5] Q. Hussain, N. Alvi, T. Latif, and S. Asghar, "Radiative heat transfer in Powell–Eyring nanofluid with peristalsis," *Int. J. Thermophys.*, vol. 40, no. 5, pp. 1–20, 2019.

[6] L. Z. Hummady, "Effect of Couple Stress on Peristaltic Transport of Powell-Eyring Fluid Peristaltic flow in Inclined Asymmetric Channel with Porous Medium," *Wasit J. Comput. Math. Sci.*, vol. 1, no. 2, pp. 106–118, 2022.

[7] P. V Satya Narayana, N. Tarakaramu, S. Moliya Akshit, and J. Ghori, "MHD flow and heat transfer of an Eyring-Powell fluid over a linear stretching sheet with viscous dissipation-A numerical study," *Front. Heat Mass Transf.*, vol. 9, no. 1, 2017.

[8] N. T. Eldabe, K. A. Kamel, S. F. Ramadan, and R. A. Saad, "Peristaltic motion of Eyring-Powell nano fluid with couple stresses and heat and mass transfer through a porous media under the effect of magnetic field inside asymmetric vertical channel," *J. Adv. Res. Fluid Mech. Therm. Sci.*, vol. 68, no. 2, pp. 58–71, 2020.

[9] S. Noreen, T. Kausar, D. Tripathi, Q. U. Ain, and D. C. Lu, "Heat transfer analysis on creeping flow Carreau fluid driven by peristaltic pumping in an inclined asymmetric channel," *Therm. Sci. Eng. Prog.*, vol. 17, p. 100486, 2020.

[10] T. S. Ahmed, "Effect of Inclined Magnetic Field on Peristaltic Flow of Carreau Fluid through Porous Medium in an Inclined Tapered Asymmetric Channel," *Al-Mustansiriyah J. Sci.*, vol. 29, no. 3, pp. 94–105, 2018.

[11] A. M. Jasim, "Study of the Impact of Unsteady Squeezing Magnetohydrodynamics Copper-Water with Injection-Suction on Nanofluid Flow Between Two Parallel Plates in Porous Medium," *Iraqi J. Sci.*, pp. 3909–3924, 2022.

[12] H. A. Ali, "Impact of Varying Viscosity with Hall Current on Peristaltic Flow of Viscoelastic Fluid Through Porous Medium in Irregular Microchannel," *Iraqi J. Sci.*, pp. 1265–1276, 2022.

[13] A. Aziz, W. Jamshed, T. Aziz, H. M. S. Bahaidarah, and K. Ur Rehman, "Entropy analysis of Powell–Eyring hybrid nanofluid including effect of linear thermal radiation and viscous dissipation," *J. Therm. Anal. Calorim.*, vol. 143, no. 2, pp. 1331–1343, 2021, doi: 10.1007/s10973-020-10210-2.

[14] R. S. Kareem and A. M. Abdulhadi, "Impacts of Heat and Mass Transfer on Magneto Hydrodynamic Peristaltic Flow Having Temperature-dependent Properties in an Inclined Channel Through Porous Media," *Iraqi J. Sci.*, pp. 854–869, 2020.

[15] A. K. Hage and L. Z. Hummady, "Influence of inclined magnetic field and heat transfer on peristaltic transfer Powell-Eyring fluid in asymmetric channel and porous medium," *Int. J. Nonlinear Anal. Appl.*, 2022.

[16] H. N. Mohaisen and A. M. Abedulhadi, "Effects of the Rotation on the Mixed Convection Heat Transfer Analysis for the Peristaltic Transport of Viscoplastic Fluid in Asymmetric Channel," *Iraqi J. Sci.*, pp. 1240–1257, 2022.